INTERNATIONAL SYMPOSIUM ON
DAMS FOR A CHANGING WORLD
-Need for Knowledge Transfer across the Generations & the World
Kyoto, Japan June 5, 2012

Development of Numerical Analysis Code for Predicting Behavior of Removal Sediment from Reservoir Bed by Using Discharge Pipe Based on Siphon Principle

N. Yoneyama
Disaster Prevention Research Institute, Kyoto University, Kyoto, Japan
yoneyama@taisui5.dpri.kyoto-u.ac.jp

A. Saito
Shikoku Research Institute Inc., Kagawa, Japan

K. Iguchi
Shikoku Electric Power Co., Inc., Kagawa, Japan

ABSTRACT:
Japan has a considerable number of dam reservoirs which have been in existence for more than 30 years, and several of these contain a considerable amount of sand sediment. Japan's electric power companies are currently studying ways to facilitate the downstream transport of sediment which has accumulated in dam reservoirs by using sediment discharge equipment based on the siphon principle. In this case, the configuration of tip of the discharge pipe can impact upon the efficiency of the sediment removal. In this study, we have developed a numerical analysis code for predicting a sediment removal behavior in order to determine the optimal configuration. The numerical results of closely matched the measurements of current and post-discharge reservoir bed configuration obtained by empirical testing. We also performed analysis on different discharge pipe tip configurations and selected a configuration which was best suited to efficient sediment removal.

Keywords: sediment, discharge equipment, numerical analysis, moving boundary method

1. INTRODUCTION

Japan has a number of dam reservoirs that are more than 30 years old, and several contain a considerable amount of sand sediment. When sand accumulates in a dam reservoir, its capacity decreases, and the downstream flow of sand declines, leading to coastal erosion.

Japan's electric power companies are currently studying ways to facilitate the downstream transport of sediment accumulated in dam reservoirs, by using sand discharge equipment based on the siphon principle. This equipment positions the discharge pipe close to the reservoir bed so that the water current can carry the sand downstream via the pipe. The configuration for the tip of the discharge pipe can impact the efficiency of the sediment removal.

In this study, we have developed a numerical analysis code for predicting a sediment removal behavior in order to determine the optimal configuration of tip of the discharge pipe.

2. NUMERICAL METHOD

The main features of the developed code are: (1) its ability to predict flows accurately in the vicinity of the discharge pipe by using an incompressible fluid analysis technique which takes turbulence into account; (2) its ability to make appropriate predictive assessments of reservoir bed erosion according to the current in the vicinity of the reservoir bed by using a moving boundary method which alters the void ratio of computational cells over time (i.e. the ratio of the feasible fluid area) ; and (3) its ability to make appropriate predictive assessments of reservoir surface behavior by using the VOF method. (Hirt et al. 1981)

2.1. Basic Equations

The basic equations for fluid flow with suspended sediment are as follows:

- Continuity equation:

$$\frac{\partial \gamma^v}{\partial t} + \frac{\partial \gamma_j^a \overline{u}_j}{\partial x_j} = 0 \tag{1}$$

- Motion equation (*i = 1, 2, 3*):

$$\frac{\partial \overline{\rho}\tilde{u}_i}{\partial t} + \frac{\gamma_j^a \tilde{u}_j}{\gamma^v}\frac{\partial \overline{\rho}\tilde{u}_i}{\partial x_j} = \overline{\rho}G_i - \frac{\partial \overline{p}}{\partial x_i} + \frac{\partial}{\gamma^v \partial x_j}\gamma_j^a\left(\mu\frac{\partial \tilde{u}_i}{\partial x_j} - \widetilde{\rho u_i'' u_j''}\right) \tag{2}$$

- Advection equation for a fluid:

$$\frac{\partial F}{\partial t} + \tilde{u}_j\frac{\partial F}{\partial x_j} = 0 \tag{3}$$

where u_i is the component of flow velocity, G_i is the external force per unit volume, p is the pressure, ρ is the density of the reservoir water, μ is the viscosity, γ^v is the void ratio of a cell, γ^a is the aperture ratio of the boundary between the cells, $\bar{}$ is the Reynolds averaging quantity, and $'$ is the fluctuation in the Reynolds averaging quantity, $\tilde{}$ is the Fabre mean quantity, and $''$ is the Fabre fluctuation, F is the fluid filling ratio of the void within a cell. We also used the following evaluation formula for the disturbed flow to calculate the Reynolds stress in Eq. 2.

- Turbulent kinetic energy equation $\left(k \equiv \overline{\rho u_i'' u_i''}/2\bar{\rho}\right)$

$$\frac{\partial \bar{\rho} k}{\partial t} + \frac{1}{\gamma^v}\frac{\partial \gamma_j^a \bar{\rho} \tilde{u}_j k}{\partial x_j} = \frac{\partial}{\partial x_j}\left[\left(\bar{\rho}\nu + \frac{\bar{\rho}\nu_t}{\sigma_k}\right)\frac{\partial k}{\partial x_j}\right] - \bar{\rho}\widetilde{u_i'' u_j''}\frac{\partial \tilde{u}_i}{\partial x_j} - \bar{\rho}\varepsilon \quad (4)$$

- Turbulent dissipation equation $\left(\varepsilon \equiv \nu \overline{\rho u_{i,j}'' u_{i,j}''}\right)$

$$\frac{\partial \bar{\rho}\varepsilon}{\partial t} + \frac{1}{\gamma^v}\frac{\partial \gamma_j^a \bar{\rho} \tilde{u}_j \varepsilon}{\partial x_j} = \frac{\partial}{\partial x_j}\left[\left(\bar{\rho}\nu + \frac{\bar{\rho}\nu_t}{\sigma_\varepsilon}\right)\frac{\partial \varepsilon}{\partial x_j}\right] - \bar{\rho}C_{\varepsilon 1}\frac{\varepsilon}{k}\widetilde{u_i' u_j'}\frac{\partial \bar{u}_i}{\partial x_j} - \bar{\rho}C_{\varepsilon 2}\frac{\varepsilon^2}{k} \quad (5)$$

where

$$-\bar{\rho}\widetilde{u_i'' u_j''} = \bar{\rho}\nu_t\left(\frac{\partial \tilde{u}_i}{\partial x_j} + \frac{\partial \tilde{u}_j}{\partial x_i} - \frac{2}{3}\frac{\partial \tilde{u}_k}{\partial x_k}\delta_{ij}\right) - \frac{2}{3}\bar{\rho}k\delta_{ij} \quad (6)$$

$$\nu_t = \begin{cases} \dfrac{C_\mu}{1+0.1B}\dfrac{k^2}{\varepsilon} & (B>0) \\ C_\mu \dfrac{k^2}{\varepsilon} & (B \le 0) \end{cases}, \quad B = -\frac{g}{\bar{\rho}}\frac{\partial \bar{\rho}}{\partial z}\Big/\left(\frac{\varepsilon}{k}\right)^2 \quad (7)$$

where ν_t is the eddy viscosity, and $\delta_{i,j}$ is the Kronecker delta. The values for the constants in Eqs. 3–6 are σ_k=1.0, σ_ε=1.3, $C_{\varepsilon 1}$=1.45, $C_{\varepsilon 2}$=1.92, and C_μ=0.09.

Basic equations for the suspended sediment as follows;

- Suspended sediment concentration transportation equation

$$\frac{\partial \bar{C}}{\partial t} + \frac{1}{\gamma^v}\frac{\partial}{\partial x_j}\gamma_j^a\left[\bar{C}\bar{u}_j + \bar{C}\bar{w}_j - \left(\beta + \frac{\nu_t}{\mathrm{Pr}_c}\right)\frac{\partial \bar{C}}{\partial x_j}\right] = 0 \quad (8)$$

- Sedimentation velocity

$$\bar{w}_3 = \frac{g}{18\nu}\frac{\rho_{sd} - \bar{\rho}}{\bar{\rho}} \quad (9)$$

where β is the suspended sediment diffusion coefficient, $(\bar{w}_j) = (0,0,-\bar{w}_3)$ is the sedimentation velocity. ρ_{sd} is the density of sediment.

And the relation between temperature T, $\bar{C}$ and $\bar{\rho}$

$$\bar{\rho} = \rho_0(T) + \left(1 - \frac{\rho_0(T)}{\rho_{sd}}\right)\bar{C} \quad (10)$$

where ρ_0 is the density of clear water. ρ_0-T relation is calculated by:

$$\rho_0(T) = 4.0705\times10^{-5}T^3 - 7.7617\times10^{-3}T^2 + 5.5301\times10^{-2}T + 999.91 \quad (11)$$

We performed calculations based on the SIMPLE method (Patankar et al., 1972) by using the discretized Eqs. 1 and 2 in the cylindrical coordinate system. The definition points for the flow velocity and the others were at the center of the boundary phase between the cells and at the centers of the cells, respectively. The discretizations of time, advective term, and others were the forward difference, third-order upwind difference, and centered difference, respectively.

Moreover, we discretized Eq. 3 based on the VOF method. We devised some countermeasures to conserve the fluid volume. (Yoneyama et al., 2007)

2.2. Moving Boundary Method

In our method, the sediment surface is recognized by using the boundary nodes and lines. The boundary nodes can move along the computation grid. If a computation cell contains both water and sediment, the cell has two boundary nodes and one boundary line. The boundary line connects those two nodes with a straight line. When the tangent velocity U_{near} near a boundary node is larger than critical velocity for sediment transport U_{cr}, the boundary node is moved downward at the constant speed V_d, where U_{cr} and V_d are parameters (Fig. 1).

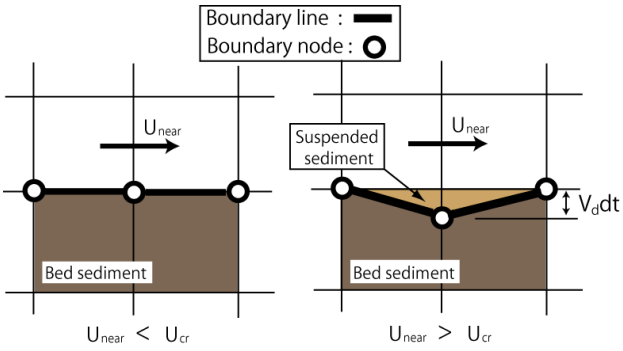

Figure 1. Procedure for moving sediment surface (1)

The slope of the sediment surface is estimated by the slope of the boundary line. When considering the effect on the angle of repose α, the higher of the two nodes is lowered at the constant speed V_d until the slope is equal to the angle of repose (Fig. 2).

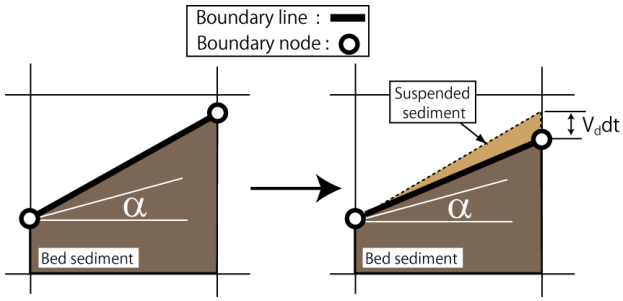

Figure 2. Procedure for moving sediment surface (2)

After determining a new sediment surface, the void ratio of a cell and the aperture ratio of the boundary between the cells are recalculated.

In this process, when a boundary point or boundary line is lowered the removed sediment is replaced to the suspended sediment. In the computation cell which contains bed boundary, a volume of the suspended sediment increases at this time. The increased volume is calculated by using the volume and the porosity of bed sediment.

2.3. Calculation Procedure

The calculation procedure is as follows:

1) Read the input data.
2) Set the boundary condition for flow velocity u_i and pressure p at time $T+dt$
3) Calculate the turbulence energy k, turbulent energy dissipation ε, and eddy viscosity ν_t at time $T+dt$.
4) Calculate the suspended sediment concentration $\bar{C}$ at time $T+dt$ by using the discretized Eq. 8.
5) Calculate the reservoir water density $\bar{\rho}$ at time $T+dt$ by using the discretized Eq. 10.
6) Calculate the location of the boundary nodes and boundary lines at time $T+dt$.
7) Calculate the void ratio γ^v and aperture ratio γ^a at time $T+dt$.
8) Recalculate the suspended sediment concentration C of the computation cell that porosity was changed.
9) Calculate the flow velocity estimate $\hat{u}_i$ at time $T+dt$ by using the discretized Eq. 2.
10) Calculate the error in the continuity equation D by using the discretized Eq. 1. If D exceeds the limit D_{max}, then correct the pressure estimate $\hat{p}$ on the basis of the solution for the pressure error equation and go back to 9). If it does not, make all of the estimates the true values and go to 11).
11) If it is time to stop, then stop the calculation. If not, increase the time and go back to 2).

3. VERIFICATION

Ashida et al. (1975) performed an experimental study on a sediment discharge system using a siphon. They measured the distributions of the flow velocities under the rigid bed condition and compared the experiment results with the potential flow analysis. They measured the shapes of the scour hole caused by the discharge flow under the movable bed condition. For verification, our code was applied to their experiments. Fig. 3 shows their experiment setup.

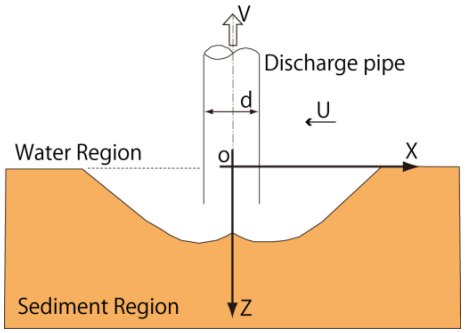

Figure 3. Experimental setup

Table 1 shows the experimental conditions that were used for the comparisons in this paper.

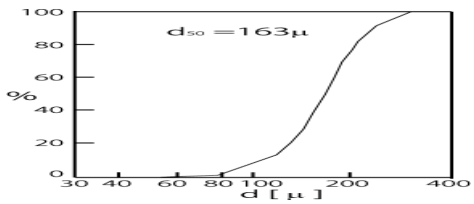

Figure 4. Grain size distribution

Fig. 4 shows the grain size distribution of the experimental sediment for the case of a movable bed. The angle of repose α for the sediment was 0.67. In their study, Ashida et al. estimated the critical velocity for transport of the experimental sediment U_{cr} to be 120 mm/s.

Table 1. Experimental Conditions

Case	d (mm)	V (mm/s)	Final position of tip of pipe Z (mm)	Rigid or movable	Initial shape of sediment surface
1	13	900	-10	Rigid	Flat
2		128	10		Final shape of Case 5
3		128	20		Final shape of Case 6
4	13	128	0	Movable	Flat
5			10		
6			20		

Fig. 5 shows the final scour hole shapes for cases 4–6.

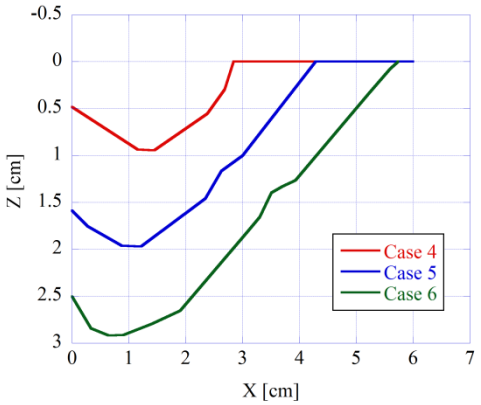

Figure 5. Scour hole shapes (Final)

3.1. Rigid Bed

First, our code was applied to Case 1. In this case, the discharge pipe is fixed, and the sediment surface is rigid. The sediment surface for Case 1 is flat. The sediment surfaces of Cases 2 and 3 were set to the final surfaces of Cases 5 and 6, respectively (Fig. 3). Fig. 6 shows the computation area.

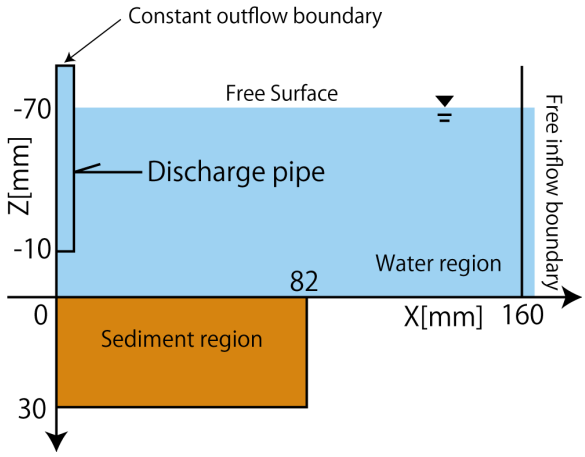

Figure 6. Computation region (2D cylindrical coordinate system)

Fig. 7 shows a snapshot of the calculated flow in Case 2.

Fig. 8 shows the vertical distribution of the horizontal velocity U at x = 4.8 cm. This figure shows a comparison between our simulation results and the experimental and potential flow analysis results conducted by Ashida et al.

Our simulation results agreed well with the experiment results. Furthermore, our results were almost identical to the potential flow analysis results except for the near-bottom region, which is difficult to simulate with the potential flow.

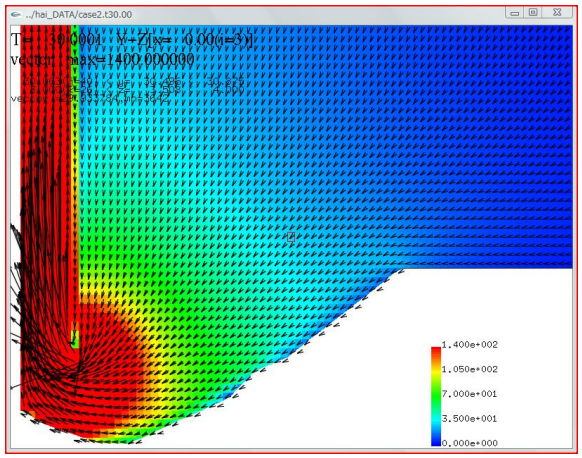

Figure 7. Snapshot of calculated flow in Case 2

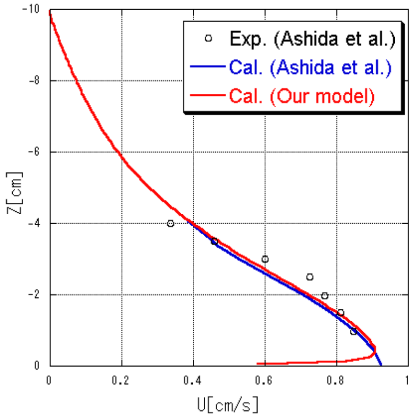

Figure 8. Vertical distribution of the horizontal velocity U

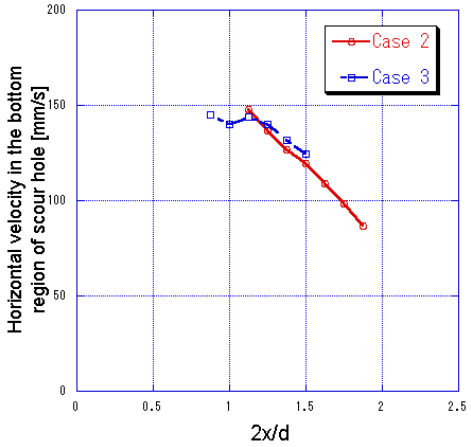

Figure 9. Horizontal velocity in near-bottom region for Cases 2 and 3

Fig. 9 shows the horizontal velocity in the near-bottom region for Cases 2 and 3. Those velocities agreed well with the critical velocity for sediment transport (120 mm/s) estimated by Ashida et al. in their study.

Thus, our code can simulate the flow toward the discharge pipe and flow in the bottom region of the scour hole.

3.2. Removable Bed

Next, our code was applied to Cases 4–6. In these cases, the discharge pipe is moved down at a speed of 1 mm/s until the final positions listed in Table 1. The initial position of the pipe tip is set to z = -10 mm. In our simulation, taking Ashida et al.'s study into account, α and U_{cr} were set to 0.67 and 120 mm/s, respectively. V_d was set to 1.0 mm/s. Fig. 10 shows snapshots of the calculated flow for Case 5.

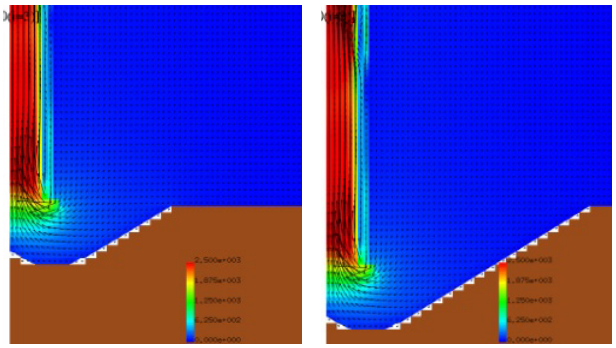

(a) T=10 s (b) T=20 s

Figure 10. Snapshots of calculated flow for Case 5

Fig. 11 shows a comparison of the scour hole shape between our simulation results and the experimental results.

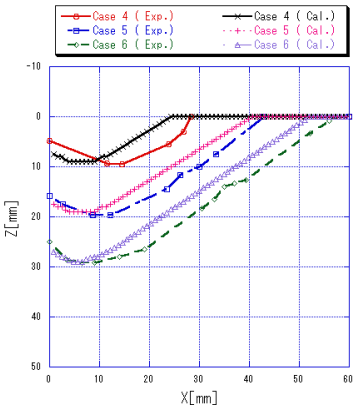

Figure 11. Comparison of scour hole shapes obtained by simulation and experiment

Our simulation results agreed well with the experimental results. Thus, our code can simulate sediment removal by a discharge pipe.

4. APPLICATION

We examined the influence of the configuration for the discharge pipe tip on the sediment removal. The configurations of the pipe tip we simulated in Cases 7–10 are shown in Fig. 12.

The initial position was z = -10 mm, constant outlet velocity V were 128 mm/s, U_{cr} and V_d were set to 120 mm/s and 1.0 mm/s, respectively. The discharge pipe was not lowered for first 10 seconds, after that it was lowered at speed of 1.0 mm/s. In Cases 7–10, the angle of repose was not considered.
Figure 13 shows a Pressure distribution for Case 9.

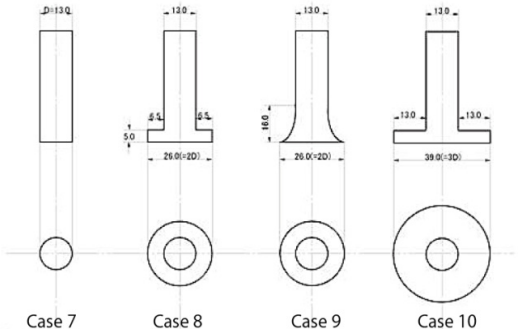

Figure 12. Configurations of pipe tip (Cases 7–10)

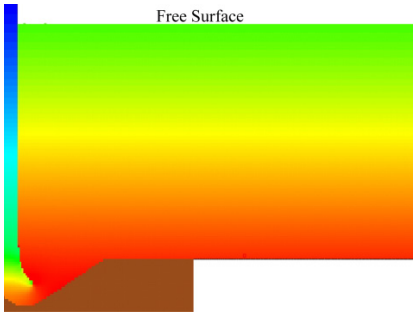

Figure 13. Snapshots of the Pressure distribution for Case 9 (red = high, blue = low)

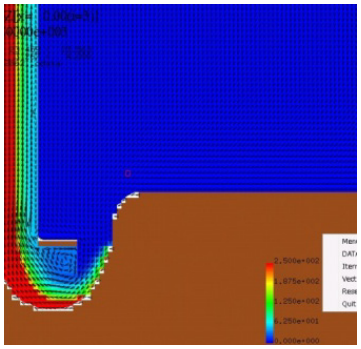

(a) Suspended sediment concentration

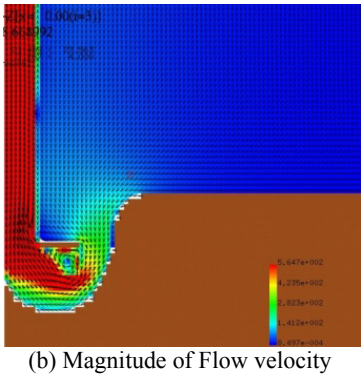

(b) Magnitude of Flow velocity

Figure 14. Snapshots of Case 8, T=20s.

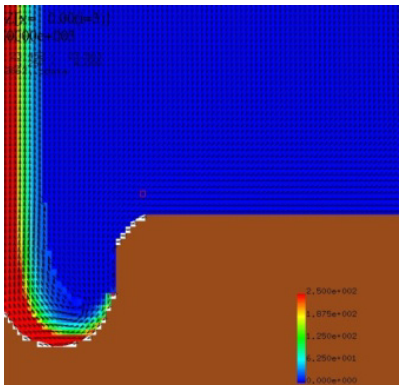

(a) Suspended sediment concentration

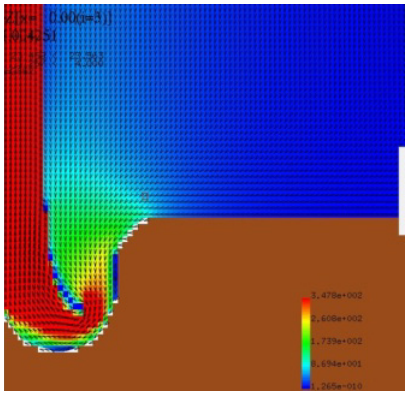

(b) Magnitude of Flow velocity

Figure 15. Snapshots of Case 9, T=20 s

Figures 14 and 15 show the snapshots of suspended sediment concentration and the magnitude of Flow velocity in the Case 8 and 9, respectively.

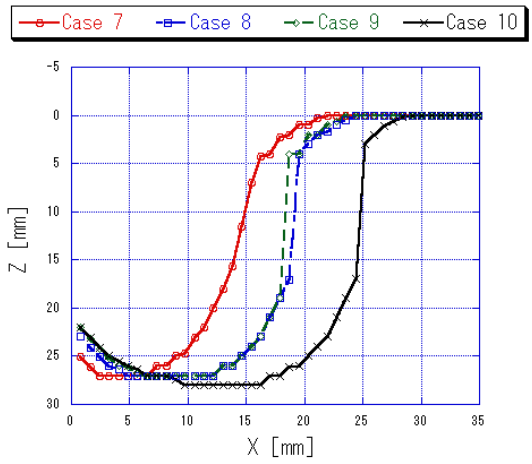

Figure 16. Snapshots of calculated flow for Case 5

Figures 16 and 17 show the calculated scour holes and total mass of the removed sediment for Cases 7–10. From those figures, the configuration for the pipe tip in Case 10 was the most efficient for sediment removal. There were few differences between Cases 8 and 9.

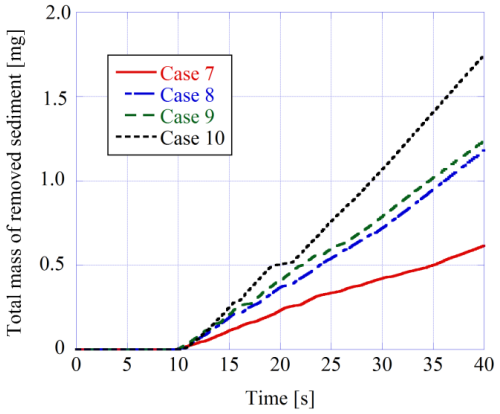

Figure 17. Total mass of the removed sediment

The results showed that removal performance improves with increasing diameter of the pipe tip.

5. CONCLUSION

We developed a numerical analysis code to predict the sand discharge behavior.

The main features of the developed code are (1) its ability to predict flows accurately in the vicinity of the discharge pipe by using an incompressible fluid analysis technique that takes turbulence into account and (2) its ability to make appropriate predictive assessments of reservoir bed erosion according to the current in the vicinity of the reservoir bed by using the moving boundary method that alters the void ratio of computational cells over time. We verified the developed code by comparing the simulation results with the experimental data collected by Ashida *et al*.

Using the code, we analyzed various tip configurations of the sediment discharge pipe. The results confirmed the applicability of our code for the determination of the optimal design of sand discharge pipes.

REFERENCES

Hirt C.W., Nichols B.D., Volume of Fluid (VOF) Method for the Dynamics of Free Boundaries, Journal of Computational Physics, Vol.39, pp.201-225, 1981.

Patankar, S.V., Spalding, D.B. (1972). A calculation procedure for heat, mass and momentum transfer in three-dimensional parabolic flow. Journal of Heat Mass Transfer 15: 1987.

Yoneyama. N., Inoue M. and Tanaka N: Three-dimensional numerical analysis for predicting the behavior of water temperature and turbidity in a pumped storage reservoir, Proc. 32st IAHR Congress, Venice, CD-ROM, 2007.

Ashida, K., Egashira, S., Matsumoto, Y. (1975). Study on sediment removal using siphon. Annual Conference of Civil Engineers, JSCE Kansai Chapter II-33: 1-2.